

Spin transport in Heisenberg antiferromagnets in two and three dimensions

M. Sentef, Marcus Kollar, Arno P. Kampf

Angaben zur Veröffentlichung / Publication details:

Sentef, M., Marcus Kollar, and Arno P. Kampf. 2007. "Spin transport in Heisenberg antiferromagnets in two and three dimensions." *Physical Review B* 75 (21): 214403. <https://doi.org/10.1103/physrevb.75.214403>.



Spin transport in Heisenberg antiferromagnets in two and three dimensions

M. Sentef, M. Kollar, and A. P. Kampf

Theoretical Physics III, Center for Electronic Correlations and Magnetism, Institute of Physics, University of Augsburg, 86135 Augsburg, Germany

(Received 21 December 2006; revised manuscript received 7 February 2007; published 1 June 2007)

We analyze spin transport in insulating antiferromagnets described by the XXZ Heisenberg model in two and three dimensions. Spin currents can be generated by a magnetic-field gradient or, in systems with spin-orbit coupling, perpendicular to a time-dependent electric field. The Kubo formula for the longitudinal spin conductivity is derived analogously to the Kubo formula for the optical conductivity of electronic systems. The spin conductivity is calculated within interacting spin-wave theory. In the Ising regime, the XXZ magnet is a spin insulator. For the isotropic Heisenberg model, the dimensionality of the system plays a crucial role: In $d=3$ the regular part of the spin conductivity vanishes linearly in the zero frequency limit, whereas in $d=2$ it approaches a finite zero frequency value.

DOI: [10.1103/PhysRevB.75.214403](https://doi.org/10.1103/PhysRevB.75.214403)

PACS number(s): 75.40.Gb, 75.10.Jm, 75.30.Ds

I. INTRODUCTION

The challenge of spintronics research is to exploit the spin degree of freedom as an additional tool in electronic devices.¹⁻⁵ This task demands to explore the basic physical principles underlying the generation and decay of spin-polarized charge currents. In this context, metallic and semi-conducting devices have been examined both theoretically and experimentally. Simultaneously, the synthesis of quasi-one-dimensional correlated insulators such as Sr_2CuO_3 (Ref. 7) and CuGeO_3 has renewed the general interest in the spin and thermal transport properties of low-dimensional quantum spin systems. Also fundamental questions have been raised, e.g., how the integrability of a system influences its spin⁸⁻¹² and thermal¹²⁻¹⁶ conductivities. In two-dimensional high-mobility electron systems with Rashba spin-orbit coupling charge currents are necessarily accompanied by spin currents.¹⁷ These spin currents flow perpendicular to the charge current direction and therefore lead to an intrinsic spin Hall effect.^{18,19}

The spin conductivity of Heisenberg chains has previously been computed within linear-response theory by adopting an analogy to the Kubo formula for charge transport.²⁰ The low-frequency behavior of the optical conductivity $\sigma(\omega) = \sigma'(\omega) + i\sigma''(\omega)$ provides a transparent scheme to distinguish the charge transport properties of ideal conductors, insulators, and nonideal conductors.^{20,21} Decomposing the real part of the longitudinal conductivity as $\sigma'(\omega) = D\delta(\omega) + \sigma^{\text{reg}}(\omega)$, a finite Drude weight or charge stiffness^{20,22} $D > 0$ is the characteristic of ideal conductors. A similar classification scheme can be carried over to spin transport and the spin conductivity in order to distinguish between spin conductors, spin insulators or even spin superfluids.^{23,24}

The optical conductivity is conveniently derived as the current response to a time-dependent electromagnetic vector potential. Similarly, for the spin current response the concept of a fictitious spin vector potential can be introduced, which is related to a twist in the direction of the spin quantization axis.²⁵ However, the physical realization of this perturbation and its relation to externally applied magnetic or electric fields is not obvious. Indeed, spin currents flow in response

to a magnetic-field gradient. In this case, the analogy to the generation of electric currents by a potential gradient is straightforwardly established for one-dimensional systems by a Jordan-Wigner transformation.²⁶⁻²⁸ This transformation maps spin- $\frac{1}{2}$ operators to creation and annihilation operators of spinless fermions; a magnetic-field gradient for the spins thereby translates into a potential gradient for the fermions.

In this paper, we do not appeal to the analogy to the charge current response. Rather, we derive the Kubo formula for the spin conductivity of XXZ Heisenberg magnets directly (Sec. II). In particular, a magnetic-field gradient or, in the presence of spin-orbit coupling,²⁹ a time-dependent electric field can be used to drive a spin current (Sec. III). The longitudinal spin conductivity of the Heisenberg antiferromagnet in two and three dimensions is computed using spin-wave theory (Sec. IV) for both the noninteracting-magnon approximation (Sec. V B) and the ladder approximation for repeated two-magnon scattering processes (Sec. V C). In particular, the low-frequency behavior of the spin conductivity will be analyzed in detail revealing distinct differences between the spin transport properties of two-dimensional (2D) and three-dimensional (3D) antiferromagnets. We find that only for an isotropic 2D antiferromagnet the spin conductivity remains finite in the dc limit.

II. KUBO FORMULA

Specifically, consider the antiferromagnetic XXZ Heisenberg model (HAFM)

$$\mathcal{H} = J \sum_{\langle i,j \rangle} \left(\Delta S_i^z S_j^z + \frac{1}{2} (S_i^+ S_j^- + S_i^- S_j^+) \right) \quad (1)$$

with nearest-neighbor exchange coupling $J > 0$, an anisotropy parameter Δ , and local spin operators \mathbf{S}_i of length S . The sum over $\langle i,j \rangle$ extends over the nearest-neighbor bonds on a d -dimensional hypercubic lattice with lattice constant $a=1$ and N sites. An external space- and time-dependent magnetic field $B^z(l,t)$ couples to the spin system via the Zeeman energy. The time-dependent Hamiltonian thus reads

$$\mathcal{H}(t) = \mathcal{H} - \sum_l S^z(l) h^z(l, t), \quad (2)$$

where $\mathbf{h}(l, t) = h^z(l, t) \mathbf{e}_z = g \mu_B B^z(l, t) \mathbf{e}_z$.

The spin current density operator $j_{i \rightarrow j}$ for the magnetization transport from site i to site j is defined via the continuity equation,

$$\partial_t S_i^z + \sum_j j_{i \rightarrow j} = 0. \quad (3)$$

Here, $\sum_j j_{i \rightarrow j}$ is the lattice divergence of the local spin current density at site i . The operator $j_x(l) = j_{l \rightarrow l+x}$ thus follows from Heisenberg's equation of motion $\dot{S}_i^z = i[\mathcal{H}, S_i^z]$ and Eq. (3) as

$$j_x(l) = \frac{J_i}{2} (S_{l+x}^+ S_l^- - S_l^- S_{l+x}^+), \quad (4)$$

where $l+x$ is the nearest-neighbor site of site l in the positive x direction. In our subsequent calculation we assume long-range antiferromagnetic order oriented along the z direction and thus restrict the analysis to a scalar spin current operator for the magnetization transport. The definition of a proper spin current vector operator $\mathbf{I}_{i \rightarrow j}$ is rather subtle, as discussed in detail in Ref. 30. In fact, if $\langle \mathbf{S}_i \rangle$ and $\langle \mathbf{S}_j \rangle$ are not collinear, only the projection of $\mathbf{I}_{i \rightarrow j}$ onto the plane spanned by the local order parameters $\langle \mathbf{S}_i \rangle$ and $\langle \mathbf{S}_j \rangle$ may be interpreted as a physical transport current. If $\langle \mathbf{S}_i \rangle$ and $\langle \mathbf{S}_j \rangle$ are collinear, however, the magnetization transport is indeed correctly described by the scalar current density operator defined in Eq. (4). We note that the proper definition of a spin current operator is also a controversial issue in the context of spin transport in semiconductors with spin-orbit coupling,³¹ but these issues are of no concern for the purpose of our analysis.

The linear spin current response to an external magnetic-field gradient is

$$\langle j_x(\mathbf{q}, \omega) \rangle = \chi_{jS}(\mathbf{q}, \omega) h^z(\mathbf{q}, \omega), \quad (5)$$

where the Fourier transforms in time and space are defined as

$$A(\mathbf{q}, \omega) = \sum_l \int_{-\infty}^{\infty} dt e^{i(\omega t - \mathbf{q} \cdot \mathbf{l})} A(l, t). \quad (6)$$

In Eq. (5) we have introduced the dynamic susceptibility

$$\chi_{jS}(\mathbf{q}, \omega) = \frac{i}{\hbar N} \int_0^{\infty} dt e^{i(\omega + i0^+)t} \langle [j_x(\mathbf{q}, t), S^z(-\mathbf{q}, 0)] \rangle. \quad (7)$$

Using the spatial Fourier transform of the continuity equation (3),

$$\dot{S}^z(\mathbf{q}, t) + i\mathbf{q} \cdot \mathbf{j}(\mathbf{q}, t) = 0, \quad (8)$$

and assuming a magnetic-field gradient of B^z only along the x direction, χ_{jS} is transformed by partial integration as

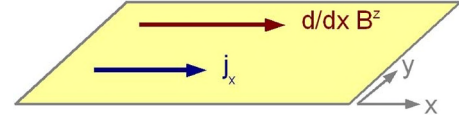


FIG. 1. (Color online) Setup for a spin current generated by a magnetic-field B^z gradient along the x direction.

$$\chi_{jS}(\mathbf{q}, \omega) = \frac{i}{\hbar N} \frac{1}{i(\omega + i0^+)} \left(-\langle [j_x(\mathbf{q}), S^z(-\mathbf{q})] \rangle + \int_0^{\infty} dt e^{i(\omega + i0^+)t} \langle [j_x(\mathbf{q}, t), i q_x j_x(-\mathbf{q}, 0)] \rangle \right). \quad (9)$$

The response formula therefore becomes

$$\langle j_x(\mathbf{q}, \omega) \rangle = -\frac{\langle -K_x \rangle - \Lambda_{xx}(\mathbf{q}, \omega)}{i(\omega + i0^+)} i q_x h^z(\mathbf{q}, \omega), \quad (10)$$

where we have introduced the spin-flip part of the exchange interaction along the x direction,

$$\langle K_x \rangle = \frac{1}{2\hbar N} \sum_l J \langle S_l^+ S_{l+x}^- + S_l^- S_{l+x}^+ \rangle, \quad (11)$$

and the longitudinal retarded current-current correlation function,

$$\Lambda_{xx}(\mathbf{q}, \omega) = \frac{i}{\hbar N} \int_0^{\infty} dt e^{i(\omega + i0^+)t} \langle [j_x(\mathbf{q}, t), j_x(-\mathbf{q}, 0)] \rangle. \quad (12)$$

For a closer analogy to charge transport, we consider the transport of magnetization $m_l = g \mu_B S_l^z$ instead of (dimensionless) spin and define the magnetization current operator $j_{m,x} = g \mu_B j_x$. The longitudinal spin conductivity $\sigma_{xx}(\omega)$ is then defined as the linear magnetization current response to a long wavelength ($\mathbf{q} \rightarrow \mathbf{0}$), frequency dependent magnetic-field gradient (Fig. 1). Setting $h^z = g \mu_B B^z$, the relation

$$j_{m,x}(\mathbf{q}, \omega) = \sigma_{xx}(\mathbf{q}, \omega) i q_x B^z(\mathbf{q}, \omega) \quad (13)$$

thus yields the Kubo formula for the spin conductivity in the long-wavelength limit,

$$\sigma_{xx}(\omega) = - (g \mu_B)^2 \frac{\langle -K_x \rangle - \Lambda_{xx}(\mathbf{q} = \mathbf{0}, \omega)}{i(\omega + i0^+)}. \quad (14)$$

This result indeed establishes the perfect analogy to the formula for the optical conductivity of interacting lattice electrons.²⁰ The real part of the spin conductivity is given by

$$\sigma'_{xx}(\omega) = D_S \delta(\omega) + \sigma_{xx}^{\text{reg}}(\omega) \quad (15)$$

with the spin stiffness^{23,24} or ‘‘spin Drude weight’’ D_S ,

$$\frac{D_S}{\pi} = (g \mu_B)^2 [\langle -K_x \rangle - \Lambda'_{xx}(\mathbf{q} = \mathbf{0}, \omega \rightarrow 0)], \quad (16)$$

and the regular part

$$\sigma_{xx}^{\text{reg}}(\omega) = \frac{\Lambda''_{xx}(\mathbf{q} = \mathbf{0}, \omega)}{\omega}. \quad (17)$$

The spin conductivity also fulfills the ‘‘ f -sum rule’’^{32,33}

$$\frac{2}{\pi} \int_0^\infty d\omega \sigma'_{xx}(\omega) = \langle -K_x \rangle, \quad (18)$$

which can be derived by using the Kubo formula and the Kramers-Kronig relations for Λ_{xx} . Note that the integral in Eq. (18) contains one-half of the possible spin Drude weight peak at zero frequency.

The structure of the spin conductivity formula emerges from the straightforward calculation for the linear current response to an external magnetic-field gradient without introducing Peierls-like phase factors with a fictitious spin vector potential.^{9,34} However, in an external electric field a moving magnetic dipole does acquire an Aharonov-Casher phase.³⁵ Katsura *et al.*²⁹ pointed out that Aharonov-Casher phase factors and a corresponding “vector potential” can be introduced on the basis of the Dzyaloshinskii-Moriya interaction,^{36,37} which may be induced in an external electric field due to spin-orbit coupling. As we show in the next section, this alternative approach leads to the same result for the spin conductivity, Eq. (14).

III. RESPONSE TO AN ELECTRIC FIELD

Spin currents are also generated by applying a time-dependent electric field in the presence of spin-orbit coupling. In low-symmetry crystals with localized spin moments spin-orbit coupling, parametrized by a coupling constant λ_{so} , leads to the Dzyaloshinskii-Moriya (DzM) antisymmetric exchange interaction^{36,37}

$$\mathcal{H}_{\text{DzM}} = \sum_{\langle ij \rangle} \mathbf{D}_{ij} \cdot (\mathbf{S}_i \times \mathbf{S}_j). \quad (19)$$

In high-symmetry crystals an inversion symmetry breaking external electric field \mathbf{E} induces a DzM vector $\mathbf{D}_{ij} \propto \mathbf{E} \times \mathbf{e}_{ij}$,³⁸ where \mathbf{e}_{ij} denotes the unit vector connecting the neighboring sites i and j . Specifically, for a field $\mathbf{E} = (0, E_y, 0)$, the DzM vector on the bonds in the x - y plane takes the form

$$\mathbf{D}_{i,i+x} = \alpha \mathbf{E} \times \mathbf{e}_x = -\alpha E_y \mathbf{e}_z, \quad \mathbf{D}_{i,i+y} = \mathbf{0}, \quad (20)$$

where $\alpha \propto \lambda_{\text{so}}$. With $(\mathbf{S}_i \times \mathbf{S}_j)^z = \frac{1}{2}(S_i^+ S_j^- - S_i^- S_j^+)$, the DzM Hamiltonian can therefore be rewritten as

$$\mathcal{H}_{\text{DzM}} = - \sum_l A_x(l, t) j_x(l), \quad (21)$$

where $j_x(l)$ is the spin current density operator defined in Eq. (4) and

$$A_x(l, t) = \frac{2\alpha E_y(l, t)}{J}. \quad (22)$$

The electric field therefore acts as a “spin vector potential” in formal analogy to the electromagnetic vector potential in charge transport.

If the DzM exchange interaction is added to the XXZ spin Hamiltonian, the Heisenberg equation of motion yields an additional contribution to the spin current operator,

$$j_{i \rightarrow j}^{\text{DzM}} = (D_{ji} - D_{ij}) \frac{1}{2} (S_i^+ S_j^- + S_i^- S_j^+), \quad (23)$$

and the total magnetization current operator is given by

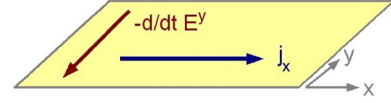


FIG. 2. (Color online) Setup for a transverse spin current driven by a time-dependent electric field in the presence of spin-orbit coupling.

$$j_{m,x}(l; A) = g\mu_B j_x(l; A=0) + (g\mu_B)^2 K_x(l) A_x(l). \quad (24)$$

As for the charge current response to an electromagnetic vector potential,²⁰ the linear spin current response to the spin vector potential in the long-wavelength limit becomes

$$\langle j_{m,x}(\mathbf{0}, \omega) \rangle = (g\mu_B)^2 [\langle K_x \rangle + \Lambda_{xx}(\mathbf{0}, \omega)] A_x(\mathbf{0}, \omega). \quad (25)$$

The spin conductivity is therefore obtained by identifying the time derivative of the spin vector potential, $i(\omega + i0^+) A_x(\mathbf{0}, \omega)$, as the driving force for the spin current. As a consequence, in the presence of spin-orbit coupling, a spin current can also be driven perpendicular to a time-dependent electric field (see Fig. 2). Physically, the origin of this phenomenon is contained in the Maxwell equation

$$\text{rot } \mathbf{B} = \frac{4\pi}{c} \mathbf{j}_c + \frac{1}{c} \frac{\partial \mathbf{E}}{\partial t}, \quad (26)$$

in the absence of charge currents, $\mathbf{j}_c = \mathbf{0}$. Assuming a magnetic field in the z direction, the y component of Eq. (26) reduces to

$$\partial_x B^z = \frac{-1}{c} \partial_t E_y = \frac{-J}{2\alpha c} \partial_t A_x. \quad (27)$$

Equation (27) identifies the time-dependent electric field and the magnetic field gradient as the same driving forces for the spin current.

IV. SPIN-WAVE THEORY FOR THE ANTIFERROMAGNETIC XXZ MODEL

In our subsequent analysis of the dynamic spin current correlation function $\Lambda_{xx}(\mathbf{0}, \omega)$ we employ interacting spin-wave theory. Even in $d=2$ and for $S=1/2$, spin-wave theory has been shown to provide quantitatively accurate results.⁴⁰ The Dyson-Maleev (DM) transformation⁴¹⁻⁴³ for the antiferromagnetic Heisenberg model on bipartite lattices is applied. In the DM representation the spin operators are replaced by bosonic operators according to

$$S_i^z = S - a_i^\dagger a_i,$$

$$S_i^+ = \sqrt{2S} \left(1 - \frac{a_i^\dagger a_i}{2S} \right) a_i, \quad S_i^- = \sqrt{2S} a_i^\dagger \quad (28)$$

for the up-spin sublattice A and by

$$S_j^z = -S + b_j^\dagger b_j,$$

$$S_j^+ = \sqrt{2S}b_j^\dagger \left(1 - \frac{b_j^\dagger b_j}{2S}\right), \quad S_j^- = \sqrt{2S}b_j \quad (29)$$

for the down-spin sublattice B . Due to the bosonic commutation relations for the a and b operators, the spin algebra is preserved.

The spatial Fourier transformation of the bosonic operators is conveniently written as⁴⁴

$$a_i = \sqrt{\frac{2}{N}} \sum_{\mathbf{k}} e^{-i\mathbf{k}\cdot\mathbf{R}_i} a_{\mathbf{k}}, \quad b_j = \sqrt{\frac{2}{N}} \sum_{\mathbf{k}} e^{+i\mathbf{k}\cdot\mathbf{R}_j} b_{\mathbf{k}}, \quad (30)$$

where the momentum \mathbf{k} is restricted to the magnetic Brillouin zone (MBZ). For the 2D square lattice MBZ = $\{\mathbf{k} : |k_x| + |k_y| \leq \pi\}$. Inserting the DM representation into the XXZ Heisenberg model, the quadratic part of the resulting bosonic Hamiltonian is diagonalized by the Bogoliubov transformation

$$a_{\mathbf{k}} = u_{\mathbf{k}}\alpha_{\mathbf{k}} + v_{\mathbf{k}}\beta_{\mathbf{k}}^\dagger, \quad b_{\mathbf{k}} = u_{\mathbf{k}}\beta_{\mathbf{k}} + v_{\mathbf{k}}\alpha_{\mathbf{k}}^\dagger. \quad (31)$$

The coefficients $u_{\mathbf{k}}$ and $v_{\mathbf{k}}$ are given by

$$u_{\mathbf{k}} = \sqrt{\frac{1 + \varepsilon_{\mathbf{k}}}{2\varepsilon_{\mathbf{k}}}}, \quad v_{\mathbf{k}} = -\text{sgn}(\gamma_{\mathbf{k}}) \sqrt{\frac{1 - \varepsilon_{\mathbf{k}}}{2\varepsilon_{\mathbf{k}}}}. \quad (32)$$

The DM transformed Hamiltonian reads

$$\mathcal{H}_{\text{DM}} = E_0 + \mathcal{H}_0 + V_{\text{DM}} \quad (33)$$

with the diagonalized quadratic part

$$\mathcal{H}_0 = \sum_{\mathbf{k}} \hbar\Omega_{\mathbf{k}} (\alpha_{\mathbf{k}}^\dagger \alpha_{\mathbf{k}} + \beta_{\mathbf{k}}^\dagger \beta_{\mathbf{k}}). \quad (34)$$

For a d -dimensional hypercubic lattice the spin-wave dispersion is

$$\hbar\Omega_{\mathbf{k}} = 2d\Delta JS\alpha(S)\varepsilon_{\mathbf{k}}, \quad \varepsilon_{\mathbf{k}} = \sqrt{1 - \gamma_{\mathbf{k}}^2/\Delta^2} \quad (35)$$

with $\gamma_{\mathbf{k}} = \frac{1}{d} \sum_{\alpha=1}^d \cos(k_\alpha)$. The magnon-vacuum energy is $E_0 = -N\Delta JS^2 \alpha^2(S)d$. The Oguchi correction factor

$$\alpha(S) = 1 + \frac{r}{2S}, \quad r = 1 - \frac{2}{N} \sum_{\mathbf{k}} \varepsilon_{\mathbf{k}}, \quad (36)$$

arises from the normal-ordering of quartic terms⁴⁵ in the interaction part V_{DM} . In $d=2$,

$$r = 1 - {}_3F_2\left(-\frac{1}{2}, \frac{1}{2}, \frac{1}{2}; 1, 1; \frac{1}{\Delta^2}\right), \quad (37)$$

with the generalized hypergeometric function ${}_3F_2$.⁴⁶ Specifically, for $d=2$, $\Delta=1$, and $S=\frac{1}{2}$, the Oguchi correction factor is given by

$$\alpha\left(\frac{1}{2}\right) = 2 - \frac{8\pi}{\Gamma\left(\frac{1}{4}\right)^4} - \frac{\Gamma\left(\frac{1}{4}\right)^4}{8\pi} \approx 1.157\,947, \quad (38)$$

where Γ denotes the gamma function. Finally, the normal-ordered quartic interaction part of the Dyson-Maleev Hamiltonian (33) reads

$$\begin{aligned} V_{\text{DM}} = & -\Delta J \frac{d}{N} \sum_{(1234)} \delta_{\mathbf{G}}(1+2-3-4) \times (V^{(1)}\alpha_1^\dagger\alpha_2^\dagger\alpha_3\alpha_4 \\ & + V^{(2)}\alpha_1^\dagger\beta_2\alpha_3\alpha_4 + V^{(3)}\alpha_1^\dagger\alpha_2^\dagger\beta_3^\dagger\alpha_4 + V^{(4)}\alpha_1^\dagger\alpha_3\beta_4^\dagger\beta_2 \\ & + V^{(5)}\beta_4^\dagger\alpha_3\beta_2\beta_1 + V^{(6)}\beta_4^\dagger\beta_3^\dagger\alpha_2^\dagger\beta_1 + V^{(7)}\alpha_1^\dagger\alpha_2^\dagger\beta_3^\dagger\beta_4^\dagger \\ & + V^{(8)}\beta_1\beta_2\alpha_3\alpha_4 + V^{(9)}\beta_4^\dagger\beta_3^\dagger\beta_2\beta_1). \end{aligned} \quad (39)$$

The interaction vertices $V^{(i)}$, $i=1, \dots, 9$ depend on the wave vectors $\mathbf{k}_1, \dots, \mathbf{k}_4$, abbreviated by $1, \dots, 4$, and are explicitly given in Ref. 39. The Kronecker delta, $\delta_{\mathbf{G}}(1+2-3-4)$, ensures momentum conservation to within a reciprocal lattice vector of the MBZ.

We briefly comment on two difficulties with the Dyson-Maleev transformation. First, two constraints, $a_i^\dagger a_i \leq 2S$ and $b_j^\dagger b_j \leq 2S$, are required for the Fock space of bosonic excitations in order to avoid unphysical spin excitations. The spin-wave analysis without constraints can nevertheless be quantitatively justified noting that $\langle a_i^\dagger a_i \rangle \approx 0.197$ in $d=2$ at $T=0$ for the $S=\frac{1}{2}$ isotropic Heisenberg model, calculated in linear spin-wave theory (LSW), where V_{DM} is neglected. This result implies for the sublattice magnetization $\langle m_A \rangle = \frac{1}{2} - \langle a_i^\dagger a_i \rangle \approx 0.303$ ($\Delta=1$), supporting *a posteriori* the validity of spin-wave theory even for $S=\frac{1}{2}$.

Second, the Dyson-Maleev transformation is not Hermitian, since $S^+ \neq (S^-)^\dagger$ when the spin operators are expressed in terms of bosonic operators. As a consequence, the quartic part of the transformed Hamiltonian is non-Hermitian, too. However, its non-Hermiticity does not affect our calculations since we will take into account the only quantitatively relevant Hermitian $V^{(4)}$ term (see Sec. V C).

V. EVALUATION OF THE SPIN CONDUCTIVITY

A. Basic propagators and correlation functions

We proceed by defining the time-ordered magnon propagators (see Refs. 39 and 44 for more details),

$$G_{\alpha\alpha}(\mathbf{k}, t) \equiv -i\langle 0 | \mathcal{T} \alpha_{\mathbf{k}}(t) \alpha_{\mathbf{k}}^\dagger(0) | 0 \rangle, \quad (40)$$

$$G_{\beta\beta}(\mathbf{k}, t) \equiv -i\langle 0 | \mathcal{T} \beta_{\mathbf{k}}^\dagger(t) \beta_{\mathbf{k}}(0) | 0 \rangle. \quad (41)$$

The bare Fourier-transformed propagators in the absence of interactions are

$$G_{\alpha\alpha}^{(0)}(\mathbf{k}, \omega) = \frac{1}{\omega - \Omega_{\mathbf{k}} + i0^+}, \quad G_{\beta\beta}^{(0)}(\mathbf{k}, \omega) = \frac{-1}{\omega + \Omega_{\mathbf{k}} - i0^+}. \quad (42)$$

The regular part of the longitudinal spin conductivity

$$\sigma_{xx}^{\text{reg}}(\omega) = (g\mu_B)^2 \frac{\Lambda_{xx}''(\mathbf{q}=\mathbf{0}, \omega)}{\omega} = -\frac{(g\mu_B)^2}{\omega} G_j''(\omega) \quad (43)$$

is determined by the imaginary part of the Fourier transformed time-ordered spin current correlation function

$$G_j(t) \equiv -\frac{i}{\hbar N} \langle 0 | \mathcal{T} j_x(t) j_x(0) | 0 \rangle \quad (44)$$

in the ground state $|0\rangle$ with the spin current operator $j_x = \sum j_x(l)$ [see Eq. (4)]. j_x is transformed by the same steps which are used for the Dyson-Maleev transformation of the HAFM Hamiltonian. The result is $j_x = j_0 + j_1$, where

$$j_0 = 2JS\alpha(S) \sum_k \sin(k_x) \times \left(\frac{\gamma_k}{\Delta \varepsilon_k} (\alpha_k^\dagger \alpha_k + \beta_k^\dagger \beta_k) - \frac{1}{\varepsilon_k} (\alpha_k^\dagger \beta_k^\dagger + \alpha_k \beta_k) \right) \quad (45)$$

and

$$j_1 = J \frac{2}{N} \sum_{(1234)} \delta_G(1+2-3-4) \sin(k_{1,x}) \times (j^{(1)} \alpha_1^\dagger \alpha_2^\dagger \alpha_3 \alpha_4 + j^{(2)} \alpha_1^\dagger \beta_2 \alpha_3 \alpha_4 + j^{(3)} \alpha_1^\dagger \alpha_2^\dagger \beta_3 \alpha_4 + j^{(4)} \alpha_1^\dagger \alpha_3 \beta_4^\dagger \beta_2 + j^{(5)} \beta_4^\dagger \alpha_3 \beta_2 \beta_1 + j^{(6)} \beta_4^\dagger \beta_3 \alpha_2^\dagger \beta_1 + j^{(7)} \alpha_1^\dagger \alpha_2^\dagger \beta_3^\dagger \beta_4 + j^{(8)} \beta_1 \beta_2 \alpha_3 \alpha_4 + j^{(9)} \beta_4^\dagger \beta_3^\dagger \beta_2 \beta_1), \quad (46)$$

where, for brevity, we have omitted here the explicit expressions of the spin current vertices $j^{(i)}$; for completeness, they are listed in the Appendix. The quadratic part j_0 is of order S^1 , but it also contains Oguchi corrections of order S^0 arising from the normal ordering of quartic terms in j_1 .

The calculation of $G_j(t)$ involves the following four correlation functions:

- (i) A two-magnon correlation function,

$$G_j^{00}(t) = -i \langle 0 | \mathcal{T} j_0(t) j_0(0) | 0 \rangle; \quad (47)$$

- (ii) a four-magnon correlation function,

$$G_j^{11}(t) = -i \langle 0 | \mathcal{T} j_1(t) j_1(0) | 0 \rangle; \quad (48)$$

- (iii) and two cross-correlation functions,

$$G_j^{01}(t) = -i \langle 0 | \mathcal{T} j_0(t) j_1(0) | 0 \rangle, \quad (49)$$

$$G_j^{10}(t) = -i \langle 0 | \mathcal{T} j_1(t) j_0(0) | 0 \rangle. \quad (50)$$

The regular part of the spin conductivity (43) is then obtained with

$$G_j(\omega) = \frac{1}{\hbar} [G_j^{00}(\omega) + G_j^{11}(\omega) + G_j^{01}(\omega) + G_j^{10}(\omega)]. \quad (51)$$

Before we continue with the calculation of $G_j(\omega)$, we discuss the selection rules for the matrix elements of the spin current operator, which provide insight into the relevant physical processes for spin transport in antiferromagnets. The Lehmann representation

$$G_j(\omega) = \frac{1}{\hbar N} \sum_n^{E_n \neq E_0} |\langle 0 | j_x | n \rangle|^2 \times \left(\frac{1}{\omega - (E_n - E_0) + i0^+} - \frac{1}{\omega + (E_n - E_0) - i0^+} \right) \quad (52)$$

shows that the spin current correlation function is determined by the matrix elements $\langle 0 | j_x | n \rangle$, where $|n\rangle$ denotes the excited states with energy E_n . The ground state and the relevant excited states must therefore have (i) the same total momentum and (ii) the same spin quantum numbers, but (iii) opposite parity in order to have nonvanishing matrix elements $\langle 0 | j_x | n \rangle$. These conditions imply that only multimagnon excitations with vanishing total momentum contribute to the spin conductivity; one-magnon excitations are forbidden by both (i) and (ii). Condition (iii) is reflected in the $\sin(k_x)$ vertex in Eq. (46), which selects the x direction for the spin current. Below we will focus on the two-magnon contribution to the spin conductivity. Apart from the $\sin(k_x)$ vertex function, our calculation proceeds analogously to the two-magnon analysis of Raman scattering in antiferromagnets.³⁹ In fact, the selection rules for spin transport are the same as for the two-magnon Raman scattering intensity in B_{1g} scattering geometry.

In the analysis of the spin current correlation function, Eq. (51), we focus on G_j^{00} because it provides the leading (S^2) order contribution and also the dominant S^1 corrections for the spin conductivity. The product $j_0(t)j_0(0)$ contains 16 terms. However, following the arguments of Canali and Girvin in Ref. 39, the contributions of 14 of these terms are negligibly small due to two arguments: First, the 12 terms containing prefactors $\gamma_k/\Delta\varepsilon_k$ are small because the absolute value of this factor is small near the MBZ boundary, where the free magnon density of states has a van-Hove singularity. Specifically, the four regions of the MBZ boundary where $|\sin(k_x)| \sim 1$ provide the quantitatively relevant contributions. Second, only two of the four remaining terms are nonzero if magnon interactions are neglected.

The two remaining dominant terms lead to

$$G_j(\omega) \approx G_j^+(\omega) + G_j^+(-\omega), \quad (53)$$

where

$$G_j^+(\omega) = \frac{[2JS\alpha(S)]^2}{\hbar N} \sum_{k,k'} \frac{\sin(k_x)\sin(k'_x)}{\varepsilon_k \varepsilon_{k'}} \Pi_{kk'}(\omega). \quad (54)$$

The two terms which are involved in Eq. (53) are thus calculated from the same two-magnon Green function,

$$\Pi_{kk'}(t) = -i \langle 0 | \mathcal{T} \alpha_k(t) \beta_k(t) \alpha_{k'}^\dagger(0) \beta_{k'}^\dagger(0) | 0 \rangle. \quad (55)$$

Its Fourier transform is expressed in terms of magnon propagators and a three-point vertex function⁴⁷

$$\Pi_{kk'}(\omega) = i \int_{-\infty}^{\infty} \frac{d\omega'}{2\pi} G_{\alpha\alpha}(\mathbf{k}, \omega + \omega') G_{\beta\beta}(\mathbf{k}, \omega') \Gamma_{kk'}(\omega, \omega'). \quad (56)$$

The vertex function $\Gamma_{kk'}(\omega, \omega')$ satisfies the Bethe-Salpeter equation

$$\begin{aligned} \Gamma_{kk'}(\omega, \omega') &= \delta_{kk'} - \frac{i}{\hbar} \frac{\Delta J d}{N} \sum_{k_1} \int_{-\infty}^{\infty} \frac{d\omega_1}{2\pi} \\ &\times \mathcal{V}_{kk_1 k_1 k}^{\alpha\beta}(\omega', \omega_1) G_{\alpha\alpha}(\mathbf{k}_1, \omega + \omega_1) \\ &\times G_{\beta\beta}(\mathbf{k}_1, \omega_1) \Gamma_{k_1 k'}(\omega, \omega_1). \end{aligned} \quad (57)$$

Here, the four-point vertex $\mathcal{V}_{kk_1 k_1 k}^{\alpha\beta}(\omega', \omega_1)$ is the sum of all the irreducible interaction parts.⁴⁷

In terms of magnon propagators and the vertex function, $G_j^+(\omega)$ is therefore given by

$$\begin{aligned} G_j^+(\omega) &= \frac{i[2JS\alpha(S)]^2}{\hbar N} \int_{-\infty}^{\infty} \frac{d\omega'}{2\pi} \sum_{\mathbf{k}} \frac{\sin(k_x)}{\varepsilon_{\mathbf{k}}} \\ &\times G_{\alpha\alpha}(\mathbf{k}, \omega + \omega') G_{\beta\beta}(\mathbf{k}, \omega') \Gamma_{\mathbf{k}}(\omega, \omega'), \end{aligned} \quad (58)$$

where the reduced vertex function $\Gamma_{\mathbf{k}}$ is defined by

$$\Gamma_{\mathbf{k}}(\omega, \omega') = \sum_{k'} \frac{\sin(k'_x)}{\varepsilon_{k'}} \Gamma_{kk'}(\omega, \omega'). \quad (59)$$

Equations (57) and (58) define the integral equations which must be solved in the calculation of the correlation function $G_j^+(\omega)$. We will proceed in two steps: In a first approximation, the interactions between magnons are omitted (Sec. V B). Subsequently, interactions are treated within a ladder approximation for repeated magnon-magnon scattering processes (Sec. V C).

B. Noninteracting magnons

We start in a first step by neglecting magnon-magnon interactions, which amounts to the replacements $G \rightarrow G^{(0)}$ and $\Gamma_{\mathbf{k}} \rightarrow \sin(k_x)/\varepsilon_{\mathbf{k}}$, i.e., $\mathcal{V}^{\alpha\beta} = 0$. The required complex contour integral in Eq. (57) then straightforwardly leads to the result

$$G_j^+(\omega) = \frac{[JS\alpha(S)]^2}{\hbar N} \sum_{\mathbf{k}} \frac{\sin^2(k_x)}{\varepsilon_{\mathbf{k}}^2} \frac{1}{\omega - 2\Omega_{\mathbf{k}} + i0^+}. \quad (60)$$

For convenience we introduce the dimensionless frequency $\tilde{\omega} = \omega/\Omega_{\max}$, where $\Omega_{\max} = 2d\Delta JS\alpha(S)/\hbar$ is the maximum one-magnon energy, and for $m \in \{0, 1, 2\}$ we define the functions

$$\ell^{(m)}(\tilde{\omega}) = \frac{2}{N} \sum_{\mathbf{k}} \frac{\sin^2(k_x)}{\varepsilon_{\mathbf{k}}^m} \frac{1}{\tilde{\omega} - 2\varepsilon_{\mathbf{k}} + i0^+}. \quad (61)$$

The regular part ($\tilde{\omega} > 0$) of the spin conductivity within LSW is then given by

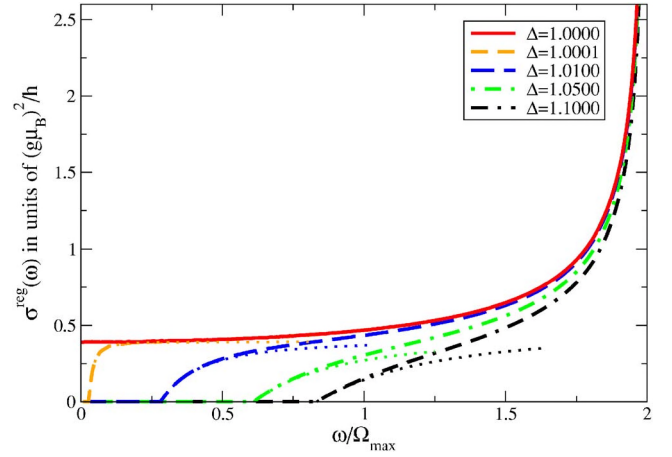


FIG. 3. (Color online) Regular part of the longitudinal spin conductivity for noninteracting magnons in two dimensions for different values of the anisotropy parameter Δ . The gap in $\sigma_{xx}^{\text{reg}}(\omega)$ increases with increasing Δ and vanishes for $\Delta=1$. The dotted lines show the expansion around ω_{gap} , Eq. (64).

$$\begin{aligned} \sigma_{xx}^{\text{reg}}(\omega) &= -\frac{(g\mu_B)^2}{h} \frac{\pi}{(d\Delta)^2 \tilde{\omega}} \text{Im} \ell^{(2)}(\tilde{\omega}) \\ &= \frac{(g\mu_B)^2}{h} \frac{\pi^2}{(d\Delta)^2 \tilde{\omega} N} \sum_{\mathbf{k}} \frac{\sin^2(k_x)}{\varepsilon_{\mathbf{k}}^2} \delta(\tilde{\omega} - 2\varepsilon_{\mathbf{k}}). \end{aligned} \quad (62)$$

Equation (62) directly reflects the spin current selection rules explained above, $\delta(\tilde{\omega} - 2\varepsilon_{\mathbf{k}})$ accounts for two magnon excitations at energy $\varepsilon_{\mathbf{k}}$. Momentum conservation and spin conservation are fulfilled by a combination of α and β magnons, which carry opposite spin ($S^z = +1$ or -1) and momentum (\mathbf{k} and $-\mathbf{k}$). In a fully polarized Heisenberg ferromagnet, there is only one magnon species and hence the spin conductivity vanishes.⁶

The spin Drude weight [Eq. (16)] $D_S = 0$ for any $\Delta \geq 1$ within LSW. Furthermore, the regular part of the spin conductivity diverges at the maximum two-magnon energy ($\tilde{\omega} = 2$) in dimensions $d=2$ and $d=3$ due to the neglect of magnon interactions. The LSW result for the spin conductivity in $d=2$ is shown in Fig. 3. A special feature of the regular part of $\sigma_{xx}^{\text{reg}}(\omega)$ is its finite zero frequency limit at the isotropic point $\Delta=1$. An expansion near the magnon energy gap $\tilde{\omega}_{\text{gap}} \equiv 2\sqrt{1 - 1/\Delta^2}$ yields the leading contribution as

$$\frac{\sigma_{xx}^{\text{reg}}(\omega)}{(g\mu_B)^2/h} \simeq \frac{\Delta^d d^{(d/2)-1} (\tilde{\omega}^2 - \tilde{\omega}_{\text{gap}}^2)^{d/2}}{2^{3d/2} \tilde{\omega}^2} \times \begin{cases} \pi, & d=2, \\ 1, & d=3, \end{cases} \quad (63)$$

for $\tilde{\omega} \geq \tilde{\omega}_{\text{gap}}$, with corrections of order $(\tilde{\omega} - \tilde{\omega}_{\text{gap}})^{(d/2)+1}$. Specifically in $d=2$, the result of the expansion is

$$\sigma_{xx}^{\text{reg}}(\omega) \simeq \sigma_{\text{LSW}}^* \Delta^2 \left(1 - \frac{\omega_{\text{gap}}^2}{\omega^2} \right) \quad (64)$$

for $\omega \geq \omega_{\text{gap}} \equiv \Omega_{\max} \tilde{\omega}_{\text{gap}}$. The finite zero frequency value of the spin conductivity for $\Delta=1$ is thus obtained as

$$\sigma_{xx}^{\text{reg}}(\omega \rightarrow 0) = \sigma_{\text{LSW}}^* = \frac{(g\mu_B)^2 \pi}{h} \frac{\pi}{8}. \quad (65)$$

The expansion (63) for the spin conductivity within LSW in $d=2$ is also shown in Fig. 3. This expansion reveals that in $d=3$, as opposed to the two-dimensional case, the spin conductivity for $\Delta=1$ vanishes linearly in the zero frequency limit within LSW (see Fig. 5). The unphysical divergence at the upper edge of the LSW spectrum will be cured by including magnon-magnon interactions as discussed in the next section.

C. Ladder approximation: two-magnon scattering

For the calculation of $G_j^+(\omega)$ magnon-magnon interactions are taken into account to lowest order³⁹ by approximating the four-point vertex $\mathcal{V}^{\alpha\beta}$ by its first-order irreducible interaction part,

$$\mathcal{V}_{kk_1k_1k}^{\alpha\beta}(\omega', \omega_1) = V_{kk_1k_1k}^{(4)}, \quad (66)$$

which is explicitly given by

$$\frac{V_{kk_1k_1k}^{(4)}}{4} = \frac{\gamma_{k-k_1}}{2} \left(\frac{1}{\varepsilon_k \varepsilon_{k_1}} + 1 \right) - \frac{\gamma_k \gamma_{k_1}}{2\Delta^2 \varepsilon_k \varepsilon_{k_1}}, \quad (67)$$

i.e., we neglect all the contributions to $\mathcal{V}^{\alpha\beta}$ where two or more of the bare interactions $V^{(i)}$ are involved. Then the magnon propagators can again be replaced by the bare expressions $G_{\alpha\alpha}^{(0)}$ and $G_{\beta\beta}^{(0)}$ in Eq. (57) since all the first-order diagrams for the magnon self-energy vanish at $T=0$.³⁹

The algebraic solution of the coupled integral equations (57) and (58) is based on the decoupling of the sums over \mathbf{k} and \mathbf{k}_1 by means of the identities

$$\sum_{\mathbf{k}} \sin(k_x) \gamma_{\mathbf{k}} g_{\mathbf{k}} = 0, \quad (68)$$

$$\sum_{\mathbf{k}} \sin(k_x) \gamma_{\mathbf{k}-\mathbf{k}_1} g_{\mathbf{k}} = \frac{\sin(k_{1,x})}{d} \sum_{\mathbf{k}} \sin^2(k_x) g_{\mathbf{k}}, \quad (69)$$

which hold for any function $g_{\mathbf{k}}$ which has the symmetry of the hypercubic lattice.

We proceed by repeatedly using Eqs. (68) and (69) to decouple Eqs. (57) and (58) leading to a ladder approximation of the Bethe-Salpeter equation for the vertex part $\Gamma_{\mathbf{k}}(\omega, \omega')$. This has been demonstrated in Ref. 39 for the vertex function $[\cos(k_x) - \cos(k_y)]/2$ of the Raman B_{1g} mode instead of the spin current vertex $\sin(k_x)$. By virtue of the identities Eqs. (68) and (69) the analogous analytical steps can be performed, and we obtain for the spin conductivity

$$\begin{aligned} \sigma_{xx}^{\text{reg}}(\omega) = & -\frac{(g\mu_B)^2}{h} \frac{\pi}{(d\Delta)^2 \bar{\omega}} \\ & \times \text{Im} \frac{\ell^{(2)} - \kappa(\ell^{(1)}\ell^{(1)} - \ell^{(0)}\ell^{(2)})}{1 + \kappa(\ell^{(0)} + \ell^{(2)}) - \kappa^2(\ell^{(1)}\ell^{(1)} - \ell^{(0)}\ell^{(2)})}, \end{aligned} \quad (70)$$

where $\ell^{(i)} \equiv \ell^{(i)}(\bar{\omega})$ and $\kappa^{-1} = 2dS\alpha(S)$.

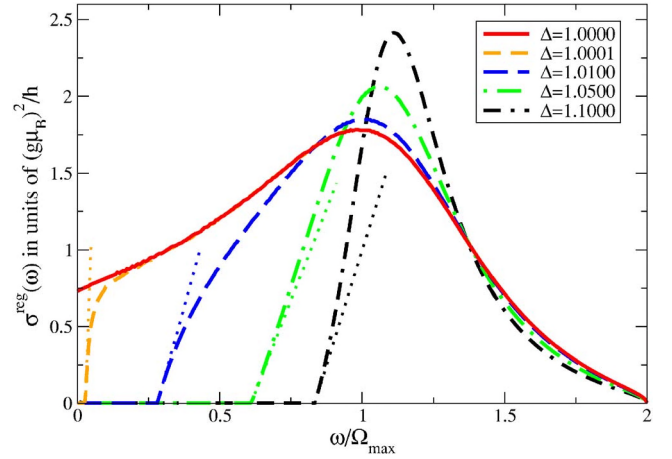


FIG. 4. (Color online) Regular part of the longitudinal spin conductivity within the ladder approximation for magnon-magnon interactions for $S=\frac{1}{2}$ in $d=2$. The gap in $\sigma_{xx}^{\text{reg}}(\omega)$ increases with increasing Δ and vanishes for $\Delta=1$. The dotted lines represent the linear expansions around ω_{gap} , Eq. (71).

Figures 4 and 5 show the $S=\frac{1}{2}$ spin conductivity within the ladder approximation for $d=2$ and $d=3$, respectively. Scattering between magnons removes the divergence of the LSW result at $\omega=2\Omega_{\text{max}}$. The frequencies for the maximal spin conductivity increase with increasing anisotropy parameter Δ .

In contrast to the spin conductivity of the 3D Heisenberg antiferromagnet, which vanishes at the isotropic point $\Delta=1$ for $\omega \rightarrow 0$, the most notable feature of the regular part of the spin conductivity of the isotropic 2D Heisenberg antiferromagnet remains its finite value in the zero frequency limit. For $\omega \geq \omega_{\text{gap}}$ we find the following leading-order linear expansion in $d=2$,

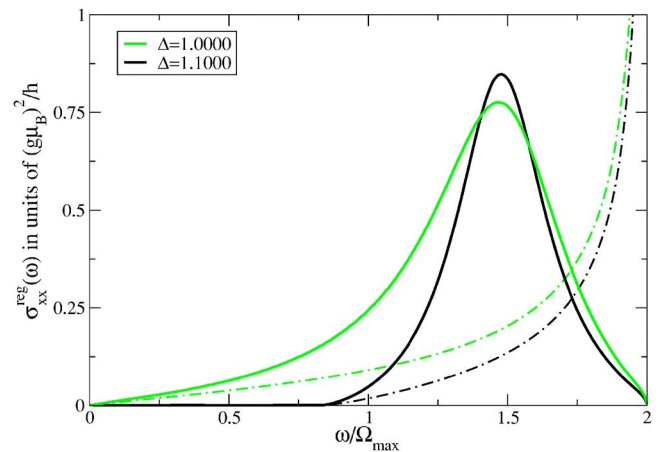


FIG. 5. (Color online) Regular part of the longitudinal spin conductivity within the ladder approximation for $S=\frac{1}{2}$ for the isotropic [green (light gray) line] and one anisotropic case (black line) in $d=3$. The dashed lines show the LSW results.

$$\sigma_{xx}^{\text{reg}}(\omega) \simeq \sigma_{\text{ladder}}^* A(\Delta) \left(1 - \frac{\omega_{\text{gap}}}{\omega}\right), \quad (71)$$

which is also included in Fig. 4. $A(\Delta)$ is a numerical prefactor with $A(1)=1$, and the zero frequency limit of the spin conductivity for $\Delta=1$ is given by

$$\sigma_{xx}^{\text{reg}}(\omega \rightarrow 0) = \sigma_{\text{ladder}}^* = Y_\sigma \frac{(g\mu_B)^2 \pi}{h} \frac{1}{8}, \quad (72)$$

$$Y_\sigma \approx 1.856\,851 \quad \text{for } S = \frac{1}{2}. \quad (73)$$

The renormalization factor Y_σ can be expressed in terms of the gamma function,

$$Y_\sigma = \frac{1 - b_0 \kappa + \frac{1}{4} b_0^2 \kappa^2}{\left[1 - \frac{1}{2}(b_0 + b_2) \kappa - \frac{1}{4}(b_1^2 - b_0 b_2) \kappa^2\right]^2}, \quad (74)$$

$$b_0 = \frac{32\pi}{\Gamma\left(\frac{1}{4}\right)^4}, \quad b_1 = 2 - \frac{4}{\pi}, \quad b_2 = \frac{\Gamma\left(\frac{1}{4}\right)^4}{4\pi^3} - \frac{16\pi}{\Gamma\left(\frac{1}{4}\right)^4}.$$

The inclusion of magnon-magnon interactions thus renormalizes σ^* from its value for noninteracting magnons. The fact that $\sigma_{xx}^{\text{reg}}(\omega)$ is finite in the limit $\omega \rightarrow 0$, however, turns out to be a robust feature of the isotropic 2D Heisenberg antiferromagnet. On the other hand, for 3D or anisotropic 2D antiferromagnets the regular part of the spin conductivity is suppressed at low frequencies.

VI. CONCLUSIONS AND OUTLOOK

In Heisenberg magnets, spin currents flow along a magnetic-field gradient or, in the presence of spin-orbit coupling, perpendicular to a time-dependent electric field. We presented an explicit derivation of the Kubo formula for the spin conductivity for the antiferromagnetic XXZ Heisenberg model and showed that the magnetization transport arises from two-magnon processes, which provide the dominant contribution to the spin conductivity.

In close analogy to the calculation of the B_{1g} two-magnon Raman light scattering intensity, the spin conductivity was evaluated using interacting spin-wave theory. The dimen-

sionality of the model is important for the low-frequency behavior of the spin conductivity, especially upon approaching the isotropic point ($\Delta=1$) from the gapped Ising regime ($\Delta > 1$). In $d=3$, the regular part of the spin conductivity vanishes for $\Delta=1$ in the dc limit. In $d=2$, however, the regular part of the spin conductivity remains *finite* for $\omega \rightarrow 0$ at the isotropic point, which separates the Ising regime from the XY regime.⁴⁸

Experimentally the spin conductivity can be determined by measurements of magnetization currents. This issue was discussed by Meier and Loss in Ref. 6, where possible experimental setups were proposed. In these setups the magnetization current is detected via the electric field which it generates. Given the estimates in Ref. 6 for the expected voltages in moderate magnetic field gradients, measurements of the spin conductivity indeed appear experimentally feasible.

ACKNOWLEDGMENT

This work was supported by the Deutsche Forschungsgemeinschaft through Sonderforschungsbereich 484.

APPENDIX: SPIN CURRENT VERTICES

The spin current vertices involved in Eq. (47) are given by

$$j^{(1)} = u_1 v_2 u_3 u_4 + v_1 u_2 v_3 v_4,$$

$$j^{(2)} = u_1 u_2 u_3 u_4 + v_1 v_2 v_3 v_4 + v_1 v_2 u_3 u_4 + u_1 u_2 v_3 v_4,$$

$$j^{(3)} = 2(u_1 v_2 v_3 u_4 + v_1 u_2 u_3 v_4),$$

$$j^{(4)} = 2(u_1 u_3 v_4 u_2 + u_1 v_3 u_4 u_2 + v_1 u_3 v_4 v_2 + v_1 v_3 u_4 v_2),$$

$$j^{(5)} = 2(v_4 u_3 u_2 v_1 + u_4 v_3 v_2 u_1),$$

$$j^{(6)} = v_4 v_3 v_2 v_1 + u_4 u_3 u_2 u_1 + v_4 v_3 u_2 u_1 + u_4 u_3 v_2 v_1,$$

$$j^{(7)} = u_1 v_2 v_3 v_4 + v_1 u_2 u_3 u_4,$$

$$j^{(8)} = v_1 u_2 u_3 u_4 + u_1 v_2 v_3 v_4,$$

$$j^{(9)} = v_4 v_3 u_2 v_1 + u_4 u_3 v_2 u_1.$$

The coefficients $u_i = u_{k_i}$ and $v_i = v_{k_i}$ with $i=1, \dots, 4$ are defined by Eq. (32).

¹S. A. Wolf, D. D. Awschalom, R. A. Buhrman, J. M. Daughton, S. von Molnár, M. L. Roukes, A. Y. Chtchelkanova, and D. M. Treger, *Science* **294**, 1488 (2001).

²*Semiconductor Spintronics and Quantum Computation*, edited by D. D. Awschalom, D. Loss, and N. Samarth (Springer-Verlag, Berlin, 2002), and references therein.

³J. C. Slonczewski, *Phys. Rev. B* **39**, 6995 (1989).

⁴The topic of spintronics was recently reviewed by I. Žutić, J. Fabian, and S. Das Sarma, *Rev. Mod. Phys.* **76**, 323 (2004).

⁵J. König, M. C. Bonsager, and A. H. MacDonald, *Phys. Rev. Lett.* **87**, 187202 (2001).

⁶F. Meier and D. Loss, *Phys. Rev. Lett.* **90**, 167204 (2003).

- ⁷M. Takigawa, N. Motoyama, H. Eisaki, and S. Uchida, *Phys. Rev. Lett.* **76**, 4612 (1996).
- ⁸X. Zotos, *Phys. Rev. Lett.* **82**, 1764 (1999).
- ⁹J. V. Alvarez and C. Gros, *Phys. Rev. Lett.* **88**, 077203 (2002); *Phys. Rev. B* **66**, 094403 (2002).
- ¹⁰S. Fujimoto and N. Kawakami, *Phys. Rev. Lett.* **90**, 197202 (2003).
- ¹¹J. Benz, T. Fukui, A. Klümper, and C. Scheeren, *J. Phys. Soc. Jpn.* **74**, 181 (2005).
- ¹²F. Heidrich-Meisner, A. Honecker, D. C. Cabra, and W. Brenig, *Phys. Rev. B* **68**, 134436 (2003).
- ¹³K. Saito, S. Takesue, and S. Miyashita, *Phys. Rev. E* **54**, 2404 (1996).
- ¹⁴A. Klümper and K. Sakai, *J. Phys. A* **35**, 2173 (2002).
- ¹⁵K. Louis and C. Gros, *Phys. Rev. B* **67**, 224410 (2003).
- ¹⁶P. Jung, R. W. Helmes, and A. Rosch, *Phys. Rev. Lett.* **96**, 067202 (2006).
- ¹⁷Y. A. Bychkov and E. I. Rashba, *J. Phys. C* **17**, 6039 (1984).
- ¹⁸S. Murakami, N. Nagaosa, and S. Zhang, *Science* **301**, 1348 (2003).
- ¹⁹J. Sinova, D. Culcer, Q. Niu, N. A. Sinitsyn, T. Jungwirth, and A. H. MacDonald, *Phys. Rev. Lett.* **92**, 126603 (2004).
- ²⁰D. J. Scalapino, S. R. White, and S. Zhang, *Phys. Rev. B* **47**, 7995 (1993).
- ²¹I. Souza, T. Wilkens, and R. M. Martin, *Phys. Rev. B* **62**, 1666 (2000).
- ²²W. Kohn, *Phys. Rev.* **133**, A171 (1964).
- ²³P. Chandra, P. Coleman, and A. I. Larkin, *J. Phys.: Condens. Matter* **2**, 7933 (1990).
- ²⁴B. S. Shastry and B. Sutherland, *Phys. Rev. Lett.* **65**, 243 (1990).
- ²⁵W. Zhuo, X. Wang, and Y. Wang, *Phys. Rev. B* **73**, 212413 (2006).
- ²⁶P. Jordan and E. Wigner, *Z. Phys.* **47**, 631 (1928).
- ²⁷E. Fradkin, *Phys. Rev. Lett.* **63**, 322 (1989).
- ²⁸D. Eliezer and G. W. Semenoff, *Phys. Lett. B* **286**, 118 (1992).
- ²⁹H. Katsura, N. Nagaosa, and A. V. Balatsky, *Phys. Rev. Lett.* **95**, 057205 (2005).
- ³⁰F. Schütz, P. Kopietz, and M. Kollar, *Eur. Phys. J. B* **41**, 557 (2004).
- ³¹J. Shi, P. Zhang, D. Xiao, and Q. Niu, *Phys. Rev. Lett.* **96**, 076604 (2006), and references therein.
- ³²P. F. Maldague, *Phys. Rev. B* **16**, 2437 (1977).
- ³³D. Baeriswyl, J. Carmelo, and A. Luther, *Phys. Rev. B* **33**, 7247 (1986).
- ³⁴R. E. Peierls, *Z. Phys.* **80**, 763 (1933).
- ³⁵Y. Aharonov and A. Casher, *Phys. Rev. Lett.* **53**, 319 (1984).
- ³⁶I. E. Dzyaloshinskii, *J. Phys. Chem. Solids* **4**, 241 (1958).
- ³⁷T. Moriya, *Phys. Rev. Lett.* **4**, 228 (1960); *Phys. Rev.* **120**, 91 (1960).
- ³⁸K. Shiratori and E. Kita, *J. Phys. Soc. Jpn.* **48**, 1443 (1980).
- ³⁹C. M. Canali and S. M. Girvin, *Phys. Rev. B* **45**, 7127 (1992).
- ⁴⁰J. I. Igarashi, *Phys. Rev. B* **46**, 10763 (1992).
- ⁴¹F. J. Dyson, *Phys. Rev.* **102**, 1217 (1956); **102**, 1230 (1956).
- ⁴²S. V. Maleev, *Zh. Eksp. Teor. Fiz.* **30**, 1010 (1957) [*Sov. Phys. JETP* **64**, 654 (1958)].
- ⁴³E. Manousakis, *Rev. Mod. Phys.* **63**, 1 (1991).
- ⁴⁴A. B. Harris, D. Kumar, B. I. Halperin, and P. C. Hohenberg, *Phys. Rev. B* **3**, 961 (1971).
- ⁴⁵T. Oguchi, *Phys. Rev.* **117**, 117 (1960).
- ⁴⁶*Handbook of Mathematical Functions*, edited by M. Abramowitz and I. A. Stegun (Dover, New York, 1972).
- ⁴⁷R. W. Davies, S. R. Chinn, and H. J. Zeiger, *Phys. Rev. B* **4**, 992 (1971).
- ⁴⁸This result indeed bears some resemblance to the “universal conductivity” at the quantum critical point in the two-dimensional boson Hubbard model at the superfluid to Mott insulator transition. See M. C. Cha, M. P. A. Fisher, S. M. Girvin, M. Wallin, and A. P. Young, *Phys. Rev. B* **44**, 6883 (1991).